Research & Reviews: Journal of Pharmacy and Pharmaceutical Sciences e-ISSN: 2320-1215

Cubic Nanoparticles as Potential Carriers for A Natural Anticancer Drug: Development, *In Vitro* and *In Vivo* Characterization

Randa Abdou[1], Mariam Mojally[2], Gouda H Attia[3], Mohamed Dawoud[4,5]*

[1]Department of Pharmacognosy, Faculty of Pharmacy, Umm Al Qura, University, Holy Makkah, KSA
[2]Department of Pharmaceutical chemistry, Faculty of Pharmacy, Umm Al Qura, University, Holy Makkah, KSA
[3]Department of Pharmacognosy, Faculty of Pharmacy, Najran University, Najran, KSA
[4]Department of Pharmaceutics, Faculty of Pharmacy, Umm Al Qura, University, Holy Makkah, KSA
[5]Department of Pharmaceutics and Industrial Pharmacy, Faculty of Pharmacy, Helwan-University, Cairo, Egypt

Research Article

Received: 24-Feb-2023, Manuscript No. JPPS-23-89981; **Editor assigned**: 27-Feb-2023, Pre QC No. JPPS-23-89981 (PQ); **Reviewed:** 13-Mar-2023, QC No. JPPS-23-89981; **Revised:** 27-Mar-2023, Manuscript No. JPPS-23-89981 (R); **Published:** 03-Apr-2023,
DOI: 10.4172/2320-1215.12.1.003

***For Correspondence:**
Mohamed Dawoud, Department of Pharmaceutics, Faculty of Pharmacy, Umm Al Qura, University, Holy Makkah, KSA
E-mail: mzdawoud@uqu.edu.sa

Citation: Dawoud M, et al. A Short Communication on Pharmacokinetic Parameters of Vancomycin used in Severe Infections in Children. RRJ Pharm Pharm Sci. 2023;12:003

ABSTRACT

Natural compounds that elicit anticancer properties are of great interest for cancer therapy. However, the low solubility and bioavailability of these compounds limit their use as efficient anticancer drugs. To avoid these drawbacks, incorporation of these compounds into cubic nanoparticles (cubosomes) was carried out. Cubosomes containing bergapten which is a natural anticancer compound isolated from *Ficus carica* were prepared by the homogenization technique using monoolein and poloxamer. These cubosomes were characterized for size, zeta potential, entrapment efficiency, small angle X-ray diffraction, *In-vitro* release, *In-vitro* cytotoxicity, cellular uptake, and antitumor activity. Particle size of cubosomes was 220 ± 3.6 nm with almost neutral zeta potential -5 ± 1.2 mV and X-ray measurements confirmed the existence of the cubic structure. Additionally, more than 90% of the natural anticancer drug was entrapped within the cubosomes. A sustained release over 30 hours was obtained for these cubosomes. Finally, these cubosomes illustrated higher *In-vitro* cytotoxicity and *In-vivo* tumor inhibition compared with the free natural anticancer compound. Thus, cubosomes could be promising carriers for enhancement of antitumor efficiency of this natural compound.

Keywords: Cubic nanoparticles; Bergapten; Natural anticancer drug; Acceptor multilamellar vesicles; *In-vitro* cytotoxicity; *In-vivo* tumor inhibition

INTRODUCTION

Cancer represents a major cause of mortality and is expected to spread annually [1]. Several studies have shown that thyroid cancer ranks the second highest cause of cancer among women in Saudi Arabia [2]. Accordingly, there is an urgent need for effective anticancer drugs. Natural products have been widely used for the treatment of many disorders including cancer [3,4]. Natural products are a very important source for the discovery and development of anticancer agents since more than 50% of the current anticancer drugs are developed from natural sources [1]. Plants are considered as a rich source of anticancer agents which can be isolated and formulated in a suitable dosage form to overcome the spread of various types of cancers.

Despite the high cytotoxic potential of most of these natural products, they exhibit poor aqueous solubility and consequently poor bioavailability which in turn diminishes their therapeutic efficiency [5,6]. Furthermore, as most anticancer drugs, they mostly exhibit toxic effects due to their non-specific distribution and poor targeting to tumor cells [7-10]. Thus, incorporation of these natural products into different lipid nanoparticles such as nanoemulsion, liposomes and solid lipid nanoparticles, is considered as an important strategy to improve their clinical performance.

Ficus species were employed in folk medicine for the treatment of many diseases such as gastrointestinal, cardiovascular, respiratory disorders and cancers [11]. Studies performed on *Ficus carica* revealed its antioxidant, cancer suppressive, and antiviral effects [12,13]. Antimicrobial activity of *F. carica* extract was reported against several bacterial strains with MIC values ranging from 0.3-5 mg/mL [14]. Additionally, antifungal activity of *F. carica* against both *C. albicans* (MIC 500 μg/mL) and *Microsporum canis* (MIC 75 μg/mL) was also proven [15]. The anticancer activity of the plant leaves extract was reported against liver cancer cells with an IC50 of 653 µg/mL [16]. Previous studies on the anticancer activity of the plant leaves' extract suggested it to be a promising source for the development of anticancer drugs. Furthermore, it was found that the main anticancer constituent of *F. carica* leaves was bergapten which exhibited cytotoxic activity against liver and stomach cancer cell lines [17]. However, bergapten has a very low aqueous solubility with a log P value equal to 2 which decreases its bioavailability and diminishes its therapeutic efficiency [5,6,18].

Nowadays, cubic nanoparticles (cubosomes) have gained a great scientific importance due to their versatile features [19-22]. These cubosomes have a unique structure that is composed of a continuous lipid bilayer enclosing water channels [23]. This unique structure gives the opportunity for these cubosomes to encapsulate drugs with different solubilities (hydrophilic or hydrophobic) [20-24]. Furthermore, biocompatibility, sustained drug release and biodegradability make cubosomes promising carriers for many types of drugs. Due to their continuous lipid bilayers, cubosomes possesses a large hydrophobic volume which allows efficient encapsulation of poor water-soluble drugs in appropriate concentrations [25,26]. Additionally, it was reported before that cubosomes are pH sensitive nanoparticles where they release their incorporated drug in the acidic environment, which is the case at the tumor site, thus increasing selectivity of the drug and reducing systemic toxicities [27]. Cubosomes showed a high

efficiency to diffuse a cross the epithelium cells which confers an advantage for drugs encapsulated within cubosomes over their free forms [28-30].

These cubic nanoparticles could be easily prepared by just mixing the lipid such as monoolein with poloxamer and water [22,23]. Therefore, these cubic nanoparticles with their small particle size and controlled drug release could be considered as favorable carriers for anticancer drugs. Cubic nanoparticles have been widely used as carriers for enhancing the anticancer activity of many chemotherapeutic agents [7, 31-33].

The aim of this study was to isolate bergapten from *F. carica* leaves extract and investigate the performance of cubosomes as carriers for this natural product. In order to isolate and purify this natural product from the plant leaves' extract in an efficient way, High-Speed Countercurrent Chromatography (HSCCC), was employed as previously reported and resulted in excellent sample recovery [34]. Upon successful purification of bergapten it was subjected to spectroscopic analysis for confirmation of its identity through comparison of obtained data with literature.

Monoolein cubosomes encapsulated bergapten were prepared by using the hot homogenization technique to obtain particles in the nanometer size range. Particle size, zeta potential, entrapment efficiency, small angle X-ray diffraction and *in-vitro* release of bergapten were determined to characterize these cubosomes. Additionally, *in-vitro* cytotoxicity and cellular uptake of these cubosomes containing bergapten were measured on mouse colorectal cells (C-26).

Finally, the antitumor activity of bergapten incorporated within these cubosomes was investigated on mice injected with colorectal (C-26) tumor. *In-vitro* cytotoxicity and tumor inhibition of these cubosomes containing bergapten were compared with those of the extract.

MATERIALS AND METHODS

Materials

Poloxamer 407 (Lutrol F127) was from BASF AG (D-Ludwigshafen), cholesterol, sucrose, tween 80 and MTT (3-(4,5-Dimethylthiazol-2-yl)-2,5-diphenyltetrazolium Bromide) were from Sigma-Aldrich (D-Steinheim), Egg Phosphatidyl Choline (EPC) was obtained from Lipoid GmbH (D- Ludwigshafen), monoolein (GMOrphic-801) from Eastman Chemical Company (Kingsport, TN), methanol was from Carl Roth GmbH (D-Karlsruhe), ethanol and chloroform all from VWR International (D-Darmstadt) , and Hepes and sodium chloride were from AppliChem GmbH (D-Darmstadt). The cell lines were purchased from ATCC, USA. All cell culture materials were purchased from Lonza Bioscience (Morristown, USA). Purified water was prepared by filtration and deionization/reverse osmosis (Milli RX20, Millipore, D-Schwalbach).

Plant collection

Ficus carica L. family Moraceae was collected from Wadi Fatima, Makkah, KSA and identified by Dr. Hany Gouda, Department of Pharmacognosy, Faculty of Pharmacy, Najran University. A voucher specimen (UQU-2019-1) of the plant is available in the herbarium, Department of Pharmacognosy, Faculty of Pharmacy, Umm al-Qura University. Dried plant leaves were powdered and extracted with petroleum ether. The obtained extract was evaporated and then subjected to separation using preparative HSCCC.

Isolation and spectroscopic analysis of bergapten

In order to determine the most suitable two-phase solvent system for bergapten its partition coefficient had to be calculated first in different solvent systems as previously described using the formula: $K = A_{upper} / A_{lower}$ where

A_{upper} is the absorbance of bergapten in the upper phase and A_{lower} its absorbance in the lower phase of the solvent system determined by calculation of the area under the peak obtained for bergapten by HPLC analysis [35]. Separation of bergapten using preparative HSCCC was carried out according to the method previously reported in literature. After successful purification of the compound it was subjected to MS and NMR analysis and its identity was confirmed by comparison of the obtained data with literature [34,35].

Cubosomes preparation

Cubosomes were prepared using 4.4% monoolein and 0.6% poloxamer 407. Poloxamer was mixed with the molten monoolein containing bergapten followed by the dropwise addition of this mixture to water under stirring for 1 day at room temperature. As reported before, these preparation procedures resulted in the formation of cubic gel which was converted to cubosomes by homogenization [23]. Consequently, this cubic gel was subjected to a homogenization process for 15 minutes at 350 bar and 40°C followed by autoclaving these homogenized dispersions at 121°C for 15 minutes [22,23,36]. Bergapten stock solution was prepared in methanol with a concentration 20 mg/ml where 500 µl from this stock solution was added to 10 ml of the homogenized monoolein dispersions followed by shaking for 3 days at 25°C to ensure complete removal of methanol [37,38].

For quantitative cellular uptake study, Nile red was used as a florescent lipid soluble dye as it was reported that the incorporation of this dye into cubosomes did not alter particle size, zeta potential and drug loading of cubosomes [7]. Florescent cubosomes were prepared by dissolving Nile red (0.15 mg/ml) in molten monoolein and completing the procedures as previously described.

Preparation of acceptor Multilamellar Vesicles (MLV)

Multilamellar Vesicles (MLV) were utilized as acceptor particles to measure the transfer of bergapten from cubosomes instead of measuring the release with the normal conventional methods which showed many drawbacks as reported before [20, 39-44]. Egg Phosphatidyl Choline (EPC) and cholesterol were dissolved in chloroform with molar ratio 4:1 (EPC: Cholesterol) [45].

After evaporating chloroform under vacuum (Büchi Rotavapor R-114, D-Essen), the remaining thin lipid film was subjected to nitrogen to ensure complete removal of chloroform. 1 ml of warm 300 mm sucrose solution was added to the lipid film and the mixture was transferred to Eppendorf tube where it was subjected to centrifugation at 5000 rpm for 10 minutes to separate MLV in the supernatant from the excess sucrose solution below. The separated MLV were washed two times with 0.5 ml HBS PH 7.4 and finally stored in HBS at refrigerator temperature.

Particle size and zeta potential measurements

Particle sizes of blank dispersions, dispersions containing bergapten and fluorescent dispersions before and after autoclaving were measured by Photon Correlation Spectroscopy (PCS) (Malvern Zetasizer Nano UK-Worcestershire) after diluting the samples with filtered demineralized water. Polydispersity Index (PDI) was determined to evaluate the homogeneity of the different dispersions. To confirm the homogeneity of these nanoparticles, particle sizes of the different monoolein dispersions and the acceptor MLV were measured using a laser diffractometer with PIDS technology (Polarization Intensity Differential Scattering), Coulter LS230 particle sizer (Beckman Coulter, D-Krefeld,). The mean volume distribution of 8 measurements was calculated using the evaluation model Mie theory.

Zeta potential is an important feature for carriers or nanoparticles containing an anticancer drug. Thus, the zeta potential of all dispersions was measured using the same Malvern instrument after diluting the samples with 10 mM tris buffer pH 7.4.

Small angle x-ray diffraction

The existence of the cubic structure and the type of the cubic phase were determined from small angle X-ray measurements of the monoolein dispersions before and after the autoclaving process. Briefly, these measurements were carried out for 1-2 h with a SWAX camera based on a Kratky collimator system (Hecus M. Braun, Optical Systems GmbH, A-Graz). From the peaks spacing ratios and the lattice parameter ($a=d\sqrt{2}$), the type of the cubic structure was determined.

Cryo Transmission Electron Microscopy (Cryo-TEM)

Without dilution, about 5 µl of cubic nanoparticles were added to a holey grid (Quantifoil Micro Tools, Jena, Germany) followed by immersing the samples into liquid ethane cooled to -170°C and -180°C in a cryobox (Carl Zeiss NTS GmbH, Oberkochen, Germany). After that, the samples were transferred with a cryotransfer unit (Gatan 626-DH) to be examined using a pre-cooled cryoelectron microscope (Philips CM120, Netherlands).

Entrapment efficiency

Ultrafiltration centrifugation technique was used to separate the excess drug from cubosomes and consequently measuring the entrapment efficiency. 1 ml of cubosomes was diluted to 10 ml with deionized water. These diluents were placed in centrifuge tubes (Amicon Ultra 3000 MWCO, Millipore, USA) followed by centrifugation for 15 min at 5000 rpm (3MK centrifuge, Sigma, Osterode, Germany).

The amount of bergapten which might be adsorbed on the membrane was determined after filtering a known concentration of bergapten solution through the membrane and measuring the drug concentration in the filtrate.

The following equation was applied to calculate the entrapment efficiency.

$$\text{EE \%} = \frac{\text{Total amount of bergapten in 1 ml cubosomes} - \text{the free bergapten}}{\text{Total amount of bergapten in 1 ml cubosomes}} \times 100\ \%$$

The amount of free bergapten is represented by the amount of bergapten in the filtrate added to the amount adsorbed by the membrane.

In-Vitro release from cubosomes

MLV were used as acceptor particles to measure the transfer of bergapten instead of measuring the release by usual conventional methods [45, 46]. To perform the transfer experiments with two lipid molar ratios 1:25 and 1:100 (cubosomes: MLV), different amounts of cubosomes containing bergapten were added to 600 µl MLV in Eppendorf tubes and the volume was completed to 1 ml with HBS. The tubes were incubated at 37°C in a shaking water bath for different time intervals. At each time interval, samples were taken and centrifuged for 15 min at 5000 rpm to separate the donor cubosomes in the supernatant as a creamy layer from the acceptor MLV as precipitant pellets. The amount of bergapten remained in the cubosomes was calculated after dissolving the separated cubosomes in methanol and measuring the UV absorbance at 221 nm. On the other hand, MLV pellets were washed twice with 250 µl HBS followed by centrifugation. After washing and centrifugation the MLV pellets were collected, dissolved in methanol and the UV absorbance was measured at 221 nm. Furthermore, the two washes were combined and dissolved in methanol followed by measuring the UV absorbance at 221 nm.

$$\%\ \text{retained} = \frac{\text{Amount of bergapten in supernatant} + \text{amount in washings}}{\text{total amount of bergapten in the cubosomes at tim 0}}\ \text{x}\ 100$$

$$\%\ \text{transferred} = \frac{\text{Amount of bergapten in MLV pellets}}{\text{total amount of bergapten in the cubosomes at tim 0}} \times 100$$

The percentage of bergapten recovery was calculated by adding both the percentage retained and transferred.

Transfer kinetics

Analysis of bergapten transfer was carried out using Microcal Origin 6.0 software where the best fitted equation for the transfer curves was:

$$A_{acc} = A_{final} - A \times e^{-k \times t} \ldots\ldots\ldots\ldots (1)$$

A_{acc} is the percentage of bergapten transferred to the acceptor MLV at time t, A_{final} is the final percentage transferred (the plateau), A is a pre-exponential coefficient and k is the transfer rate constant.

In-vitro cytotoxicity

Cytotoxicity of cubosomes containing bergapten was studied on colorectal cells (C-26) using MTT assay. These cells were cultured in RPMI 1640 medium which contained 10% Fetal Bovine Serum (FBS) in addition to streptomycin (100 µg/ml), penicillin (100 units/ml) and 0.25 µg/ml amphotericin B at 37°C and 5% CO_2. The cells were seeded (3000 cells/well) in a 96-well plate at 37°C and 5% CO_2 for 24 hours. These cells were treated with blank cubosomes, cubosomes containing bergapten and free bergapten solution for 48 and 72 hours. After removing the old medium, MTT solution was added and incubated with the cells for 4 hours to form formazan crystals. The percentage cell viability was calculated after adding Dimethyl Sulfoxide (DMSO) to each well and measuring the UV absorbance at 570 nm. Finally, IC_{50} (concentration of bergapten inhibits cell growth by 50%) was determined from the percentage viability (y-axis) and log concentrations (x-axis).

Cellular uptake

C-26 cells were seeded in 24-well plate at a density of 105 cells/well followed by incubating them with the fluorescent cubosomes for different time periods. Afterwards, cells were washed several times with cold PBS in order to remove excess cubosomes. The percentage of the fluorescent cubosomes that have been taken by the cells was calculated using the flow cytometer (Epics XL-MCL, Beckman Coulter Inc., US-Fullerton) after diluting the samples with PBS in a measurement tube [47]. The count rate was 250 events/second and after 10,000 events the measurements were stopped. The detection was carried out at photomultiplier tube number 4 (FL4) with a detection wavelength range of 665-685 nm. Between each measurement, cleaning of the device was performed to avoid contamination of particles of preceding samples. Imaging and visualization of the cells were carried out using the microscope Zeiss Axio (Zeiss, Germany) [7].

Antitumor activity

The animal studies protocols were approved from the ethics committee at the Faculty of Pharmacy, Umm Al Qura University with approval number (UQU-Pharmacy, 1200). The animal experiments were carried out according to EU Directive 2010/63/EU for animal experiments. In the shaved right flank of male mice with average weight 18-20 g and age 5 weeks, C-26 cells were injected. After 1 week, the mice were distributed randomly into 4 groups (5 mice/group). Different amounts of blank cubosomes, cubosomes containing bergapten, free bergapten solution and 5% dextrose were injected into the mice tail through intravenous route followed by measuring the tumor size using a digital caliper [48, 49]. After 22 days the mice were scarified, and the tumor weight was measured. Mice lost more than 15% of their body weight and those with a tumor volume greater than 1000 mm^3 were excluded from the experiments.

Statistical analysis

Statistical analysis was performed using Student's t-test. The differences between the results were significant when the p values were smaller than 0.05.

RESULTS

Characterization of cubosomes

For successful targeting and retention of cubosomes in the tumor cells, cubosomes should possess particle size in the nanometer size range [50,51]. Accordingly, monoolein cubosomes were prepared by the homogenization technique which led to the formation of monoolein dispersions with a particle size of 100 ± 1.3 nm as seen in figure 1. Unfortunately, these dispersions which are prepared by the homogenization technique usually possess a vesicular structure rather than the cubic one. After autoclaving, particle size increased to 230 ± 2.4 nm due to fusion of these vesicular particles to form the cubic structure shown in Figure 1 [23-36]. Additionally, the visual observation of these monoolein dispersion confirmed the particle size measurements since translucent dispersions were obtained before autoclaving which became milky dispersions after the autoclaving process.

Figure 1. PCS z-average mean particle size (bars) and Polydispersity Indices (PDI, circles) of blank monoolein dispersions, monoolein dispersions containing bergapten, and monoolein dispersions containing Nile red before and after autoclaving, (n=3).

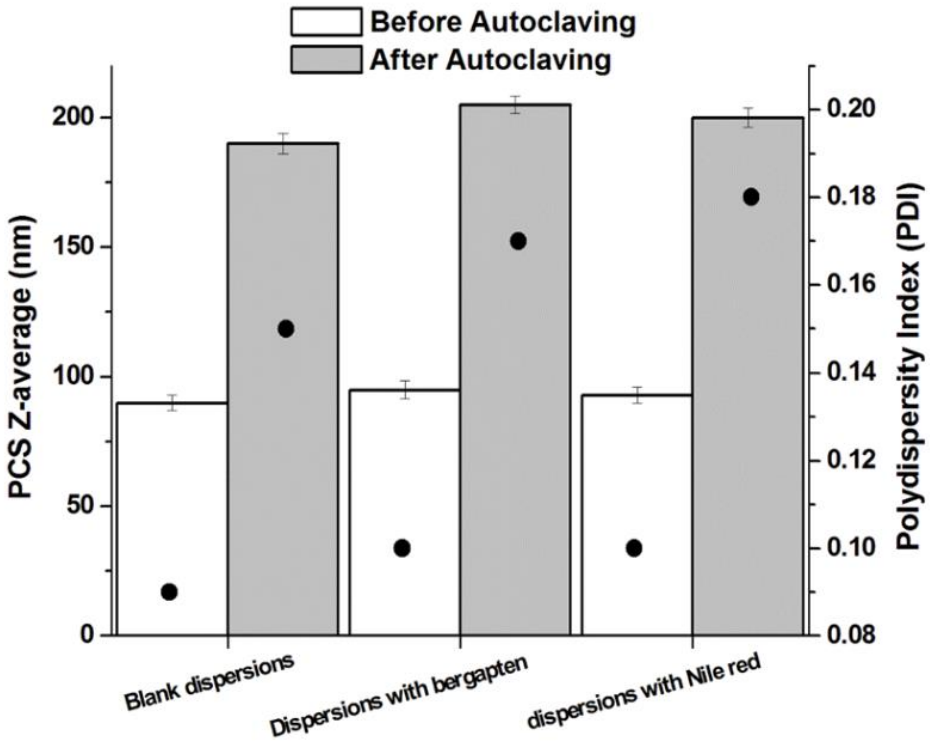

As illustrated in figure 1, incorporation of bergapten or florescent dye Nile red did not alter particle size of the dispersions. Furthermore, the Polydispersity Index (PDI) of all dispersions was less than 0.2 which indicates the homogeneity of these dispersions. In addition to the importance of particle size for targeting nanoparticles, zeta potential also plays an important role in the uptake of nanoparticles by tumor cells [52-54]. Figure 2 show that all the prepared dispersions possessed a slightly negative zeta potential ranging from -2 to -5 mV.

Figure 2. Zeta potential of blank monoolein dispersions, monoolein dispersions containing bergapten, and monoolein dispersions containing Nile red before and after autoclaving, (n=3).

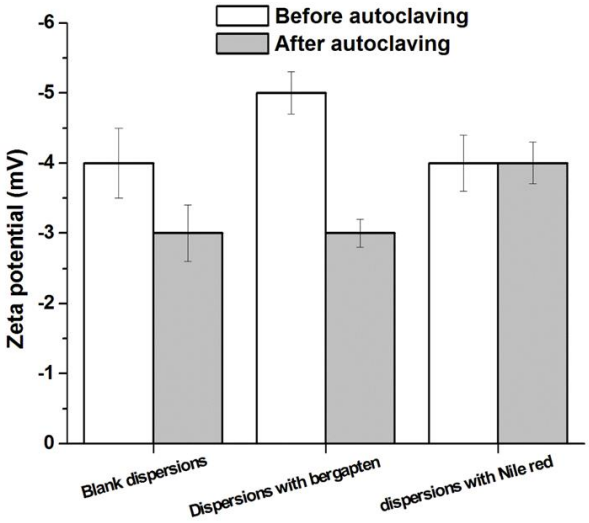

To confirm the absence of any particles in the micrometer size range for all cubic dispersions, particle sizes were measured using the laser diffractometry technique. The results obtained from this technique confirmed the previously obtained results from the photon correlation technique where no particles were observed in the micrometer size range and a small increase in the particle size was observed after the autoclaving process (Figure 3).

Figure 3. LD-PIDS particle size distribution of the monoolein dispersions containing bergapten (before and after autoclaving) and the acceptor MLV.

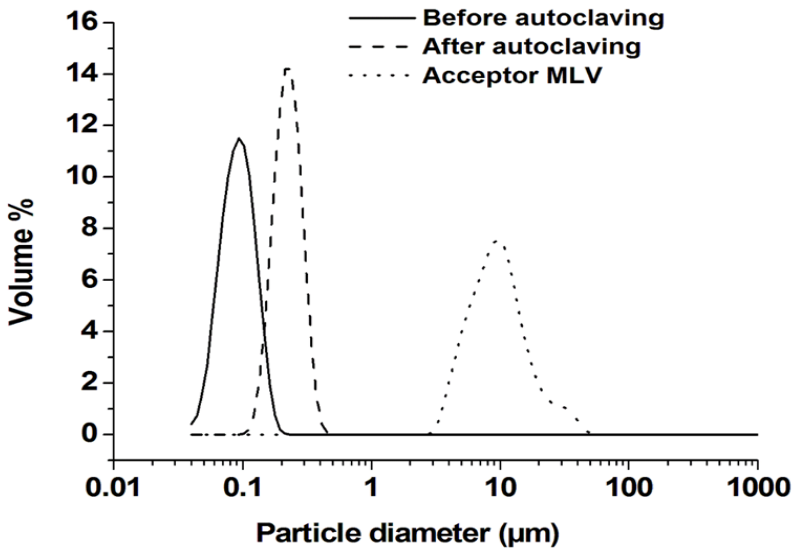

Additionally, the presence of a monomodal particle size distribution as seen in Figure 3 indicates the homogeneity of these cubic dispersions. On the other hand, particle size of the acceptor MLV was about 10 µm as illustrated in Figure 3 where these acceptor particles were not subjected to any size reduction process.

The dispersions after autoclaving show the characteristic X-ray reflections of P-type cubic phase which is recognized through a lattice parameter of 14 nm and the presence of three peaks with the spacing ratios of √2:√4:√6 (Figure 4).

Figure 4. Small angle X-ray diffractograms of monoolein dispersions containing bergapten before and after autoclaving, S=1/d (d is spacing of the reflection observed).

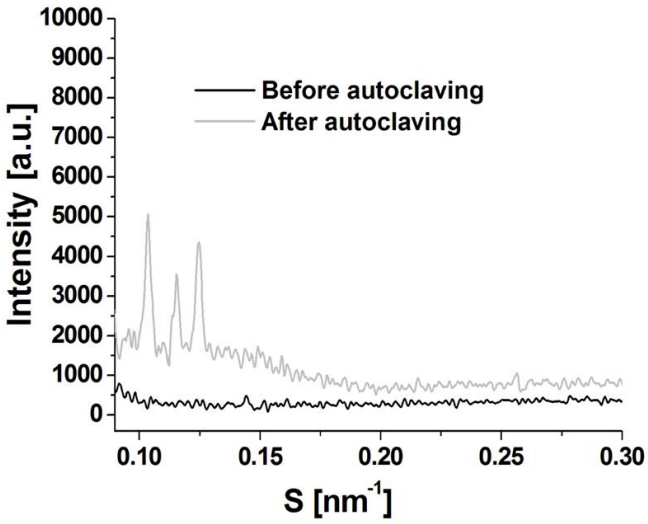

On the contrary, no reflections were observed before the autoclaving process which indicates the absence of the cubic structure for all dispersions before the autoclaving process.

The cryo-TEM pictures confirmed the presence of cubic structure of the prepared monoolein nanoparticles with a particle size slightly more than 200 nm as observed before from particle size measurements (Figure 5).

Figure 5. Cryo transmission electron microscopy (cryo-TEM) images of cubosomes.

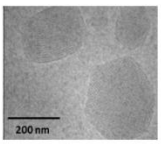

The entrapment efficiency of bergapten into the cubosomes was 93% ± 3.5. The transfer of bergapten from the donor cubosomes to the acceptor MLV was characterized by 2 phases. A rapid transfer was observed in the first phase where about 15% and 23% were transferred to the acceptor MLV in the first hour with lipid molar ratios of 1:25 and 1:100 (donor cubosomes: acceptor MLV), respectively. As shown in Figure 6a-6b, a second slow phase of transfer was observed in which about 90% and 95% were transferred after 30 hours with lipid molar ratios 1:25 and 1:100, respectively.

Figure 6. Transfer of bergapten from the donor monoolein cubosomes to the acceptor MLV with lipid molar ratio 1:25 and 1:100). a) %bergapten transferred to the acceptor MLV; b) %bergapten retained in the donor monoolein cubosomes, (n=3).

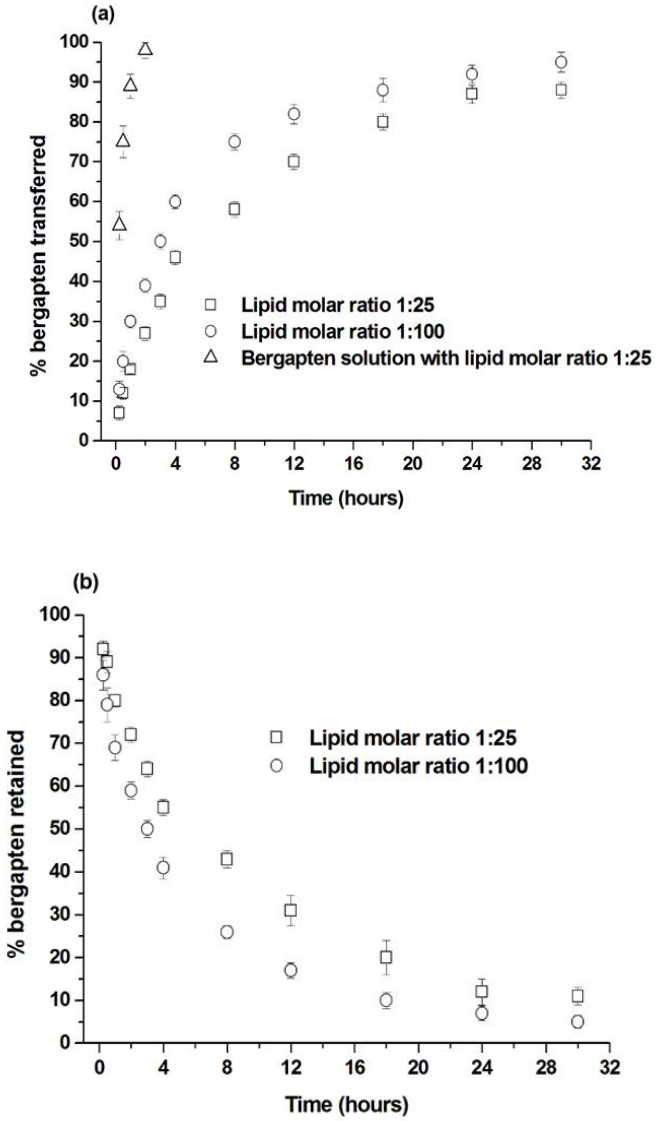

This slow or sustained transfer over a wide period is very important for any nanoparticles intended to be used as carriers for anticancer drug to achieve a successful treatment. On the contrary, the transfer of bergapten from its solution was very fast and completed after 1 hour with a transfer rate constant of about 1.44 ± 0.24 h^{-1} in case of lipid molar ratio 1:25. As expected, increasing the number of the acceptor MLV in the transfer medium led to a rapid transfer rate where the transfer rate constant K was 0.09 ± 0.018 h^{-1} for lipid molar ratio 1:25 and by increasing this ratio to 1:100 the value of K increased to 0.19 ± 0.016 h^{-1} as illustrated in Table 1. On the other hand, the percent recovery (sum of percent retained and transferred) was 99% ± 2.5 which indicates the success of this transfer technique in measuring the release of bergapten.

Table 1. Kinetic parameters derived from fits to the transfer curves of bergapten from the donor cubosomes to the acceptor MLV assuming transfer kinetics according to equation [1].

Donor: Acceptor lipid molar ratio	Donor	Transfer rate constant K (h^{-1})	Final % transferred	Equilibrium time	R^2 for fitting
1:25	Cubosomes	0.09 ± 0.018	90 ± 3.1	30	0.991
	Solution	1.44 ± 0.24	98 ± 2.3	1	0.992
1:100	Cubosomes	0.19 ± 0.016	95 ± 2.5	32	0.991

In-vitro cytotoxicity and cellular uptake

The percentage viability of C-26 cells after 48 and 72 hours of exposure to cubosomes containing bergapten, blank cubosomes and free bergapten solution is demonstrated in Figure 7a-7b.

Figure 7. Cytotoxicity of bergapten cubosomes, bergapten solution and blank cubosomes on C-26 cell lines after 48, and 72-h exposure to 0.01-100 µM samples by MTT assay, a) after 48 hr, b) after 72 hr, (n=3).

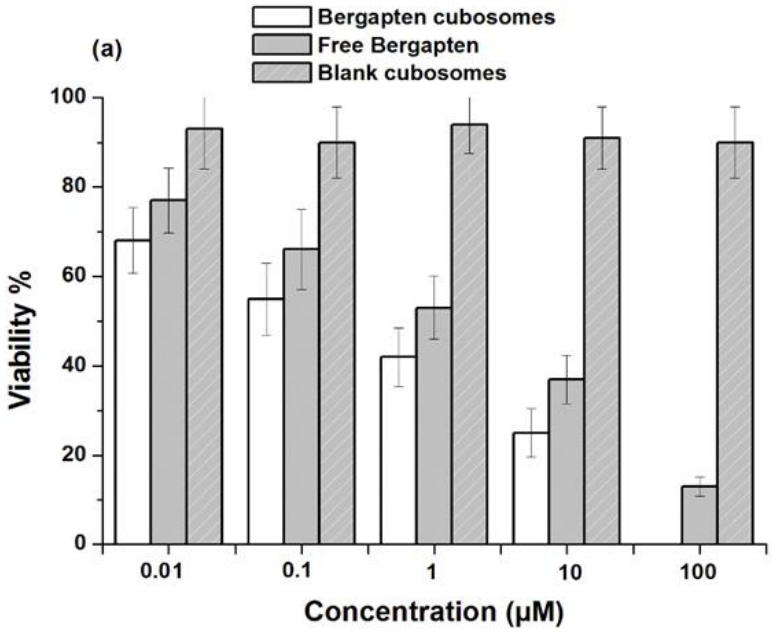

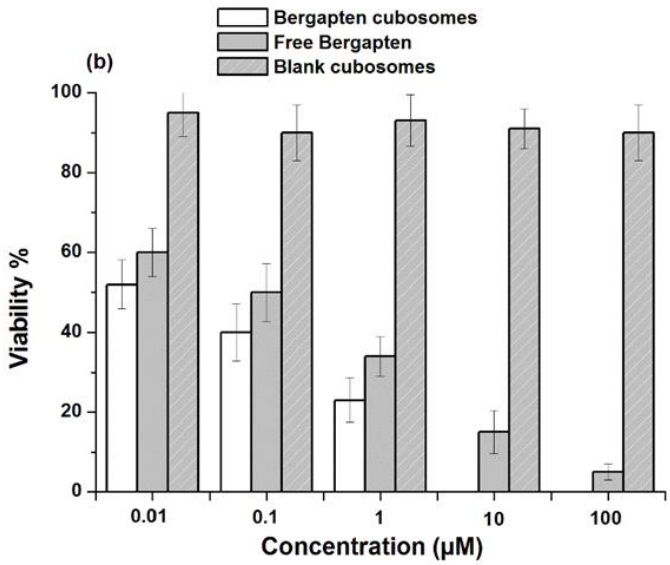

More than 90% viability was observed with the blank cubosomes which means that any observable cytotoxic effect for the cubosomes containing bergapten was related to this compound and not to the cubosomal compositions or components. No survival was observed after 48 hours of exposure to 100 μM of cubosomes containing bergapten while about 13% viability was obtained with the same concentration of bergapten solution as illustrated in Figure 7a. Increasing the exposure time to 72 hours led to the death of all cells at a concentration of 10 μM for cubosomes containing bergapten. On the contrary, about 15% and 5% of the cells still survived after 72 hours of exposure to 10 μM and 100 μM of bergapten solution, respectively as observed in Figure 7b. IC_{50} values confirmed these results as illustrated in Table 2 where smaller concentrations of the cubosomes containing bergapten were required to inhibit the growth of C-26 cells by 50% compared to bergapten solution. After 48 hours of exposure to bergapten cubosomes about 0.19 ± 0.004 μM was needed to kill 50% of C-26 cells while about 0.64 ± 0.017 μM of bergapten solution was required to kill the same percentage of these cells which indicates the higher *in-vitro* cytotoxicity of bergapten cubosomes compared to bergapten solution. These results were in agreement with the previously reported results which showed a higher *in-vitro* cytotoxicity of the anticancer drugs incorporated into different lipid nanoparticles compared with the free solutions of these anticancer drugs [51,55].

Table 2. IC_{50} (μM) for bergapten cubosomes and bergapten solution on C-26 Cell Lines after 48 and 72 hours.

IC_{50} (μM)	48 h	72 h
Bergapten cubosomes	0.19 ± 0.004	0.015 ± 0.001
Bergapten solution	0.64 ± 0.017	0.062 ± 0.003

The percentage of cellular uptake of florescent cubosomes, which were prepared with the lipid soluble dye Nile red, increased with increasing incubation time to reach about 95% after 24 hours of incubation as seen in Figure 8a-8b.

Figure 8. The cellular uptake of fluorescent cubosomes in C-26 cell lines at different time points, a) quantitative cellular uptake percentage was measured using flow cytometer (n=3), b) qualitative uptake was monitored using the microscope Zeiss Axio.

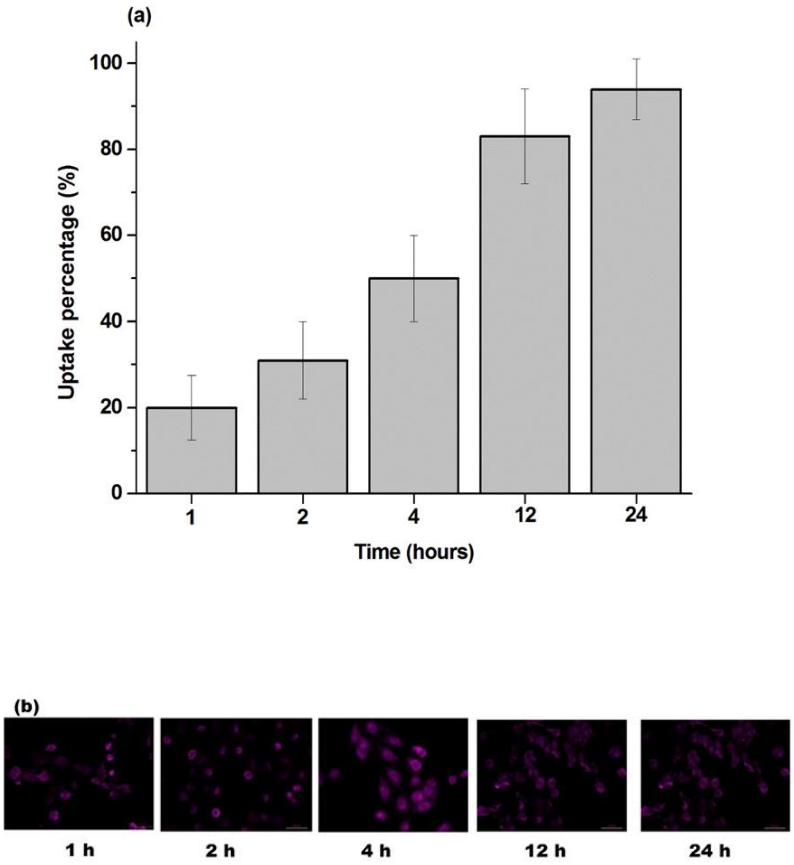

Antitumor activity

Monitoring of the tumor volume within 22 days of the experiment revealed that both cubosomes containing bergapten and bergapten solution inhibited tumor growth. However, cubosomes showed more significant inhibition than the solution ($p<0.01$) since tumor volumes at the end of the study (after 22 days) were 275 mm^3 and 490 mm^3 for cubosomes and solution, respectively (Figure 9).

Figure 9. Tumor inhibitory efficacy of bergapten cubosomes, bergapten solution, blank cubosomes and 5% dextrose, (n=5).

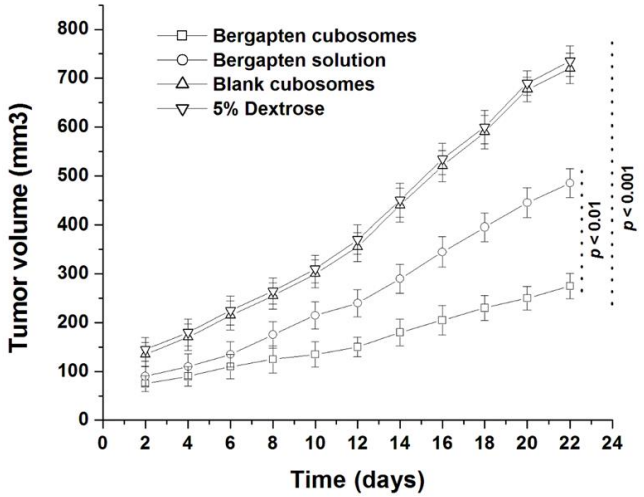

Furthermore, the average tumor weight after 22 days in mice injected with cubosomes was about 290 mg which was much lower than the weight in mice injected with the solution (510 mg) as seen in Figure 10a-10b.

Figure 10. *In vivo* anti-tumor activity after intravenous injection of bergapten cubosomes, bergapten solution, blank cubosomes and 5% dextrose, a) the weights of tumors at the end of the study, b) photographs of tumors developed in mice receiving various treatments at the end of the study, (n=5).

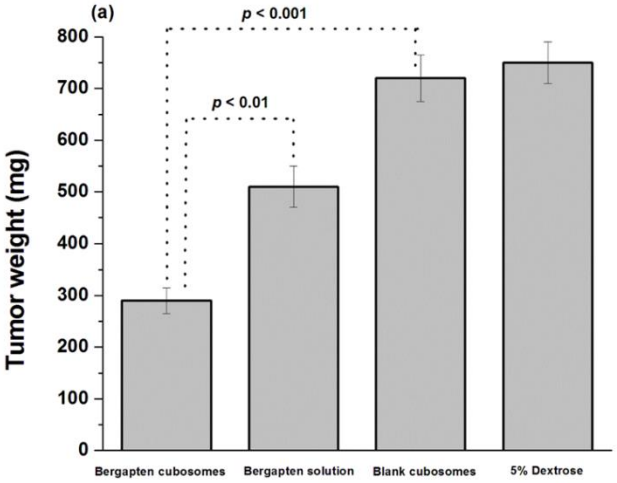

The smallest tumor size and weight after receiving bergapten cubosomes were confirmed from the photographic images of the different tumors at the end of the study (Figure 10b). Both tumor volume and weight demonstrated the stronger antitumor activity of bergapten incorporated into cubosomes than in solution.

DISCUSSION

Anticancer drugs from natural origins are of great importance as they are obtained from natural sources and are free from any synthetic materials; however this advantage cannot ensure their successful use in the treatment of cancer [56-58]. One of the techniques which has been used previously to improve the efficiency of these natural anticancer drugs is their incorporation into suitable nanocarriers such as liposomes and solid lipid nanoparticles [59-62]. For successful treatment, these carriers should have certain specifications such as small particle size and controlled drug release. Accordingly, monoolein cubic nanoparticles or cubosomes were chosen as carriers for the natural anticancer compound, bergapten as they usually have a small particle size and release the incorporated drug in a controlled manner [22, 55, 63]. Additionally, it was reported that monoolein cubic nanoparticles were safe, biocompatible, and stable [64-65]. Furthermore, monoolein cubosomes can be easily prepared by just mixing monoolein with poloxamer and water followed by shaking for 1 day [23, 36].

Cubosomes were prepared by the homogenization technique to obtain particles in the nanometer size range, however it was reported that this technique led to the formation of a vesicular structure rather than cubosomes [23] and an autoclaving process was required to fuse these vesicles to form cubosomes. Thus, the autoclaving step in the preparation of cubosomes was essential to achieve the required cubic structure. This cubic structure and the effect of the autoclaving process was observed from X-ray measurements where the peaks of the cubic phase were demonstrated only after the autoclaving step. The neutral surface charge of these cubosomes was intended and required to achieve a perfect interaction between these neutral cubosomes and the negative cell membrane [58, 59, 66].

Since the conventional release methods (dialysis based assay and continuous flow method) showed many drawbacks such as blockage of the filter and the use of aqueous release medium, the transfer of bergapten from donor cubosomes to acceptor MLV was carried out. The poor aqueous solubility of bergapten which is less than 1 mg/ml, hinders the measurement of its release using the different conventional techniques. Furthermore, these acceptor MLV with their composition (EPC and cholesterol) were very similar to the cell membranes and other lipophilic components present in the blood [46,67,68]. Consequently, these transfer experiments give a good prediction on the *in-vivo* performance and behavior of these cubosomes.

The fusion of monoolein vesicles to form cubosomes gives a unique structure for these cubosomes which extends as a lipid bilayers network and acts as a sponge like structure. Thus, a very high percentage of more than 90% of bergapten was entrapped within the cubosomes. From the release point of view, it was biphasic where it started rapidly within the first hour followed by a sustained transfer over the remaining experimental periods. This transfer behavior could be explained by the localization of the drug at different places in the cubosomes. Drug molecules at the cubosomal surfaces were responsible for the rapid initial release or transfer, while drug molecules within the continuous lipid bilayer's network or the sponge structure were slowly transferred and were responsible for the second controlled release phase. Increasing the number of the acceptor particles in the transfer medium by increasing lipid molar ratio from 1:25 to 1:100 led to a faster transfer rate while the final amount transferred was almost the same with both molar ratios which indicates the perfect sink conditions that had been achieved with these transfer experiments. The results of the *in-vitro* cytotoxicity confirmed the high safety of the cubosomes due

to their biocompatible compositions. The observed cytotoxicity was attributed to the presence of the natural anticancer drug.

Cubosomes exhibited a higher and significant cytotoxic effect than the drug solution ($p<0.05$) due to the ability of cubosomes to entrap and retain inside cancer cells. The main reason for this was the presence of cubosomal continuous phospholipid bilayers which facilitated the interaction with the phospholipid bilayers of the cell membranes [7]. Consequently, the attachment, entrance, and cellular uptake of the cubosomes containing bergapten were higher than the free drug solution. Moreover, these phospholipid bilayers might inhibit P-glycoprotein (P-gp efflux mechanism) which in turn increased the retention and accumulated these cubosomes inside the cells [69-71]. The results of antitumor activity agreed with *in-vitro* cytotoxicity as these cubosomes showed a high ability to enter and accumulate inside the tumor cells. Thus, the anticancer activity of bergapten was augmented by its incorporation within the cubosomes.

CONCLUSION

Cubic nanoparticles or cubosomes are at the forefront of lipid nanoparticles due to their unique structure and the ease of their preparations. Cubosomes could incorporate successfully bergapten which is a natural anticancer drug isolated from the leaves of *Ficus carica*. Encapsulating bergapten within cubosomes led to releasing it slowly in a controlled manner which is an important property for successful treatment using any anticancer drug. Furthermore, incorporating bergapten within cubosomes improved its *in-vitro* cytotoxicity and *in-vivo* antitumor activity compared to bergapten solution. Accordingly, cubosomes could be considered as promising carriers for such natural anticancer drugs.

ACKNOWLEDGEMENT

Funding

The author would like to thank the Deanship of Scientific Research at Umm Al-Qura University for supporting this work by Grant code: 23UQU4350488DSR02

Authors' contributions

Mohamed Dawoud: Conceptualization, Methodology, Writing - Original Draft, Project administration, Investigation

Randa Abdou: Methodology, Funding acquisition, Review & Editing

Mariam Mojally: Methodology, Resources

Availability of data and material

All data are included in the manuscript

Conflicts of interest

The authors report no conflicts of interest. The authors alone are responsible for the content and writing of this article

REFERENCES

1. Twilley D, et al. The role of natural products from plants in the development of anticancer agents. Natural Products and Drug Discovery. 2018: 139-178.
2. Alharbi MH, et al. Association of menstrual and reproductive factors with thyroid cancer in Saudi female patients. JUMS. 2021;7:11-13.
3. Wang Z, et al. Photoacoustic cavitation-ignited reactive oxygen species to amplify peroxynitrite burst by photosensitization-free polymeric nanocapsules. Angew Chem Int Ed Engl. 2020;60:4720-4731.

4. Lu Y, et al. Bioresponsive materials. Nat. Rev. Mater. 2016;2:1-17.
5. Chen Y, et al. An UPLC-MS/MS method for determination of solasonine in rat plasma and its application of a pharmacokinetic and bioavailability study. J Chromatogr B. 2015;985:1-5.
6. Zheng X, et al. Quantitative determination and pharmacokinetic study of solamargine in rat plasma by liquid chromatography–mass spectrometry. J Pharm Biomed Anal. 2011;55:1157-1162.
7. Mehanna MM, et al. Anticancer activity of thymoquinone cubic phase nanoparticles against human breast cancer: Formulation, cytotoxicity and subcellular localization. Int J Nanomedicine. 2020;15:9557-9570.
8. Ong YS, et al. Thymoquinone loaded in nanostructured lipid carrier showed enhanced anticancer activity in 4T1 tumor-bearing mice. Nanomedicine. 2018;13:1567-1582.
9. El-Aziz E, et al. The potential Of optimized liposomes in enhancement of cytotoxicity and apoptosis of encapsulated Egyptian propolis on hep-2 cell line. Pharmaceutics. 2021:13.
10. Shawky AM, et al. Pharmacophore-based virtual screening, synthesis, biological evaluation, and molecular docking study of novel pyrrolizines bearing urea/thiourea moieties with potential cytotoxicity and CDK inhibitory activities. J Enzyme Inhib Med Chem. 2021;36:15-337.
11. Vieira LM, et al. Naturally-occurring xanthones: recent developments. Curr Med Chem. 2005;12:2413-2446.
12. Herre EA, et al. Evolutionary ecology of figs and their associates: Recent progress and outstanding puzzles. Annu Rev Ecol Evol Syst. 2008;39:439-458.
13. Joseph B, et al. Pharmacognostic and phytochemical properties of *Ficus carica* linn- an overview. Int J Pharmtech Res. 2011;3:8-12.
14. Joeng MR, et al. Antimicrobial activity of methanol extract from *Ficus carica* leaves against oral bacteria. J Bacteriol Virol. 2009;39:97-102.
15. Aref HL, et al. *In vitro* antimicrobial activity of four *Ficus carica* latex fractions against resistant human pathogens (antimicrobial activity of *Ficus carica* latex). Pak J Pharm Sci. 2010;23:53-58.
16. Purnamasari R, et al. Anticancer activity of methanol extract of *Ficus carica* leaves and fruits against proliferation, apoptosis and necrosis in Huh7it cells. Cancer Informatics. 2019;18:1-7.
17. Zhang Y, et al. Extracts and components of *Ficus carica* leaves suppress survival, cell cycle, and migration of triple-negative breast cancer MDA-MB-231 cells. Onco Targets and Therapy. 2018;11:4377-86.
18. Said A, et al. Lipophilicity determination of psoralens used in therapy through solubility and partitioning: Comparison of theoretical and experimental approaches. J Pharm Sci. 1996;85:387-392.
19. Bei D, et al. Formulation of dacarbazine-loaded cubosomes. Part III. Physicochemical characterization. AAPS PharmSciTech. 2010;11:1243-1249.
20. Boyd BJ. Characterisation of drug release from cubosomes using the pressure ultrafiltration method. Int J Pharm. 2003;260:239-247.
21. Clogston J, et al. Controlling release from the lipidic cubic phase by selective alkylation. J Control Release. 2005;102: 441-461.
22. Dawoud MZ, et al. Comparison of drug release from liquid crystalline monoolein dispersions and solid lipid nanoparticles using a flow cytometric technique. Acta Pharm Sin. 2016;6:163-169.
23. Barauskas J, et al. Cubic phase nanoparticles (Cubosome): Principles for controlling size, structure, and stability. Langmuir. 2005;21:2569-2577.

24. Verma P, et al. Cubic liquid crystalline nanoparticles: Optimization and evaluation for ocular delivery of tropicamide. Drug Deliv. 2016;23:3043-3054.
25. Mohyeldin SM, et al. Superiority of liquid crystalline cubic nanocarriers as hormonal transdermal vehicle: Comparative human skin permeation-supported evidence. Expert Opin Drug Deliv. 2016;13:1049-1064.
26. Murgia S, et al. Drug-loaded fluorescent cubosomes: Versatile nanoparticles for potential theranostic applications. Langmuir. 2013;29: 6673-6679.
27. Kluzek M, et al. Influence of a pH-sensitive polymer on the structure of monoolein cubosomes. Soft Matter. 2017;13:7571-7577.
28. Gan L, et al. Self-assembled liquid crystalline nanoparticles as a novel ophthalmic delivery system for dexamethasone: Improving preocular retention and ocular bioavailability. Int J Pharm. 2010;396:179-187.
29. Li J, et al. A potential carrier based on liquid crystal nanoparticles for ophthalmic delivery of pilocarpine nitrate. Int J Pharm. 2013;455:75-84.
30. Siemann DW, et al. The unique characteristics of tumor vasculature and preclinical evidence for its selective disruption by tumor-vascular disrupting agents. Cancer Treat Rev. 2011;37:63-74.
31. Cytryniak A, et al. Lipidic cubic-phase nanoparticles (cubosomes) loaded with doxorubicin and labeled with (177) Lu as a potential tool for combined chemo and internal radiotherapy for cancers. Nanomaterials. 2020:10.
32. Nazaruk E, et al. Lipidic cubic-phase nanoparticles-cubosomes for efficient drug delivery to cancer cells. Chempluschem. 2017;82:570-575.
33. Zewail M, et al. Lipidic cubic-phase leflunomide nanoparticles (cubosomes) as a potential tool for breast cancer management. Drug Deliv. 2022;29:1663-1674.
34. Hua-Bin L, et al. Preparative isolation and purification of bergapten and imperatorin from the medicinal plant *Cnidium monnieri* using high-speed counter-current chromatography by stepwise increasing the flow-rate of the mobile phase. J Chromatogr A. 2004;1061:51-4.
35. Chunyan C, et al. Isolation and purification of psoralen and bergapten from *Ficus carica* L. leaves by high-speed countercurrent chromatography. J Liq Chromatogr Relat. 2009;32:136-143.
36. Dawoud M, et al. Monoolein cubic nanoparticles as novel carriers for docetaxel. J Drug Deliv Sci Technol. 2020:56.
37. Goke K, et al. Parameters influencing the course of passive drug loading into lipid nano emulsions. Eur J Pharm Biopharm. 2018;126:123-131.
38. Petersen S, et al. Flow cytometry as a new approach to investigate drug transfer between lipid particles. Mol Pharmaceutics. 2010;7:350–363.
39. D'Souza SS, et al. Development of a dialysis *in vitro* release method for biodegradable microspheres. AAPS Pharmscitech. 2005;6:323-328.
40. D'Souza SS, et al. Methods to assess *in vitro* drug release from injectable polymeric particulate systems. Pharm Res. 2006;23:460-474.
41. Levy M Y M, et al. Drug release from submicronized o/w emulsion - a new *in vitro* kinetic evaluation model. Int J Pharm. 1990;66:29-37.
42. Washington C. Evaluation of non-sink dialysis methods for the measurement of drug release from colloids - effects of drug partition. Int J Pharm. 1989;56:71-74.
43. Washington C. Drug release from microdisperse systems: A critical review. Int J Pharm. 1990;58:1-12.

44. Magenheim B, et al. A new *in-vitro* technique for the evaluation of drug-release profile from colloidal carriers - ultrafiltration technique at low-pressure. Int J Pharm. 1993;94:115-123.
45. Shabbits JA, et al. Development of an *in vitro* drug release assay that accurately predicts *in vivo* drug retention for liposome-based delivery systems. J Control Release. 2002;84:161-170.
46. Dawoud M, et al. Comparative study on the suitability of two techniques for measuring the transfer of lipophilic drug models from lipid nanoparticles to lipophilic acceptors. AAPS PharmSciTech. 2014;15: 1551-1561.
47. Ibuki Y, et al. Nanoparticle uptake measured by flow cytometry. Methods Mol Biol. 2012;926:157-166.
48. Sloat BR, et al. *In vitro* and *in vivo* anti-tumor activities of a gemcitabine derivative carried by nanoparticles. Int J Pharm. 2011;40:88-278.
49. Yanasarn N, et al. Nanoparticles engineered from lecithin-in-water emulsions as a potential delivery system for docetaxel. Int J Pharm. 2009;379:174-180.
50. Mosallaei N, et al. Docetaxel-loaded solid lipid nanoparticles: Preparation, characterization, *in vitro*, and *in vivo* evaluations. J Pharm Sci. 2013;102:1994-2004.
51. Naguib YW, et al. Solid lipid nanoparticle formulations of docetaxel prepared with high melting point triglycerides: *in vitro* and *in vivo* evaluation. Mol Pharm. 2014;11:1239-1249.
52. Eid HM, et al. Development, optimization, and *in vitro/in vivo* characterization of enhanced lipid nanoparticles for ocular delivery of ofloxacin: The influence of pegylation and chitosan coating. AAPS Pharm Sci Tech. 2019;20:183.
53. Prado-Audelo MLD, et al. Chitosan-decorated nanoparticles for drug delivery. J Drug Deliv Sci Technol. 2020:59.
54. Piazzini V, et al. Solid lipid nanoparticles and chitosan-coated solid lipid nanoparticles as promising tool for silybin delivery: Formulation, characterization, and *in vitro* evaluation. Curr Drug Deliv. 2019;16:142-152.
55. Meli V, et al. Docetaxel-loaded fluorescent liquid-crystalline nanoparticles for cancer theranostics. Langmuir. 2015;31:9566-9575.
56. Adewale OB, et al. Investigation of bioactive compounds in *Crassocephalum rubens* leaf and *in vitro* anticancer activity of its biosynthesized gold nanoparticles. Biotechnol Rep. 2020;28:560.
57. Karamchedu S, et al. Morin hydrate loaded solid lipid nanoparticles: Characterization, stability, anticancer activity, and bioavailability. Chem Phys Lipids. 2020;233:104988.
58. Sultana S, et al. Nanoparticles-mediated drug delivery approaches for cancer targeting: a review. J Drug Target. 2013;21:107-125.
59. Baek JS, et al. Surface modification of solid lipid nanoparticles for oral delivery of curcumin: Improvement of bioavailability through enhanced cellular uptake, and lymphatic uptake. Eur J Pharm Biopharm. 2017;117:132-140.
60. Chen J, et al. Fabrication and evaluation of curcumin-loaded nanoparticles based on solid lipid as a new type of colloidal drug delivery system. Indian J Pharm Sci. 2013;75:178-184.
61. Sun J, et al. Curcumin-loaded solid lipid nanoparticles have prolonged *in vitro* antitumour activity, cellular uptake and improved *in vivo* bioavailability. Colloids Surf B Biointerfaces. 2013;111:367-375.
62. Hu Q, et al. Recent advances of cocktail chemotherapy by combination drug delivery systems. Adv Drug Deliv Rev. 2016;98:19-34.

63. Bender J, et al. Lipid cubic phases for improved topical drug delivery in photodynamic therapy. JCR. 2005;106:350-360.
64. Amar-Yuli I, et al. Solubilization of food bioactives within lyotropic liquid crystalline mesophases. Curr Opin Colloid Interface Sci. 2009;14:21-32.
65. Chang CM, et al. Swelling of and drug release from monoglyceride-based drug delivery systems. J Pharm Sci. 1997;86:747-752.
66. Yu S, et al. Chitosan and chitosan coating nanoparticles for the treatment of brain disease. Int J Pharm. 2019;560:282-293.
67. Dawoud M. Transfer of a lipophilic drug model from lipid nanoparticle carriers to a lipophilic acceptor compartment. Am J PharmTech Res. 2013;3:370.
68. Dawoud M. Investigations on the transfer of porphyrin from o/w emulsion droplets to liposomes with two different methods. Drug Dev Ind Pharm. 2015;41:156-162.
69. Maeda H, et al. Polymeric drugs for efficient tumor-targeted drug delivery based on EPR-effect. Eur J Pharm Biopharm. 2009;71:409-419.
70. Simon S, et al. Inhibitory effect of phospholipids on P-glycoprotein: Cellular studies in Caco-2, MDCKII mdr1 and MDCKII wildtype cells and P-gp ATPase activity measurements. Biochim Biophys Acta. 2012;1821: 1211-1223.
71. Zhou M, et al. Overcoming chemotherapy resistance *via* simultaneous drug-efflux circumvention and mitochondrial targeting. Acta Pharm Sin B. 2019; 9:615-625.